

Effect of oxygen on characteristics of nickel oxide/indium tin oxide heterojunction diodes

Hung-Lu Chang, T. C. Lu, H. C. Kuo, and S. C. Wang

Citation: *Journal of Applied Physics* **100**, 124503 (2006); doi: 10.1063/1.2404466

View online: <http://dx.doi.org/10.1063/1.2404466>

View Table of Contents: <http://scitation.aip.org/content/aip/journal/jap/100/12?ver=pdfcov>

Published by the [AIP Publishing](#)

Articles you may be interested in

[Near-ideal electrical properties of InAs/WSe₂ van der Waals heterojunction diodes](#)

Appl. Phys. Lett. **102**, 242101 (2013); 10.1063/1.4809815

[Fabrication of zinc oxide nanorods based heterojunction devices using simple and economic chemical solution method](#)

Appl. Phys. Lett. **93**, 083124 (2008); 10.1063/1.2975829

[Fabrication and photoresponse of a pn -heterojunction diode composed of transparent oxide semiconductors, p-NiO and n- ZnO](#)

Appl. Phys. Lett. **83**, 1029 (2003); 10.1063/1.1598624

[Fabrication of transparent p–n heterojunction thin film diodes based entirely on oxide semiconductors](#)

Appl. Phys. Lett. **75**, 2851 (1999); 10.1063/1.125171

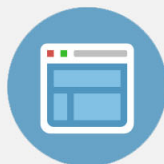
[Fabrication of n -type nickel doped B 5 C 1+ homojunction and heterojunction diodes](#)

Appl. Phys. Lett. **70**, 1028 (1997); 10.1063/1.118434



Re-register for Table of Content Alerts

Create a profile.



Sign up today!



Effect of oxygen on characteristics of nickel oxide/indium tin oxide heterojunction diodes

Hung-Lu Chang, T. C. Lu,^{a)} H. C. Kuo, and S. C. Wang
*Institute of Electro-Optical Engineering, National Chiao Tung University, Hsinchu,
 30050 Taiwan, Republic of China*

(Received 21 June 2006; accepted 20 October 2006; published online 19 December 2006)

p-nickel oxide (NiO_x)/*n*-indium tin oxide heterostructure *p-n* junction diodes were fabricated on glass substrates and showed rectifying characteristics or negative differential resistance (NDR) characteristics depending on the content of oxygen in the NiO_x films. After annealing the heterojunction diodes at 450 °C in air for about 30 min, the characteristics of NDR disappeared and transparent rectifying diodes were observed. The oxygen content could be observed by inspecting the characteristics of the NiO_x films before and after annealing using x-ray photoelectron spectrum and thermogravimetric analysis as well as atomic force microscopy. The released oxygen in the NiO_x films could be responsible for the disappearance of NDR characteristics and the change of the nonideal rectifying diode characteristics. © 2006 American Institute of Physics.
 [DOI: 10.1063/1.2404466]

I. INTRODUCTION

The diversity in oxide semiconductor junctions and their functions were rather limited compared to conventional semiconductors, even though oxide semiconductors have excellent stability in harsh environments and have unique functions such as optical transparency, chemical sensing,¹ as well as photoluminescence. For exploiting the full potential of oxide semiconductors, the combination of a *p*-type oxide semiconductor with a *n*-type oxide semiconductor has been made for electronic and optoelectronic applications, such as rectifying diodes, transistors, photodetectors, and light-emitting diodes.^{2–6} Most oxide semiconductors have *n*-type properties because cation interstitials (donors) are formed much more easily than anion interstitials (acceptors). Therefore, synthesizing *p*-type oxide-based semiconductors is a major challenge in forming *p-n* junctions. Transition metal oxides, such as Li-doped NiO (Ref. 7) and Cu-related oxide compounds,^{8–10} are exceptional because these oxides are generally *p*-type semiconductors, since the transition metal ions can be easily oxidized with the consequent formation of Ni and Cu vacancies. Like Li-doped NiO, excess O₂ in the NiO film has similar properties and is also a *p*-type semiconductor. Although the conducting mechanism in the NiO has long been the subject of much controversy, resistivity of the NiO film can be lowered by an increase of the Ni³⁺ ions resulting from the excess oxygen in the NiO crystallite.⁷ Recently, NiO-related and oxide-based heterojunction with characteristics of rectifying and photon sensing has also been reported.^{5,6,11} These innovative materials and applications are pushing the progress of oxide-based semiconductors steadily.

In this work, the *p-n* heterojunction diodes based on the nickel oxide (NiO_x)/indium tin oxide (ITO)/glass were fabricated with different ratios of O₂ in the sputtered NiO_x films on the same ITO glass. *I-V* curves of *p-n* heterojunction

diodes exhibit the characteristics of negative differential resistance (NDR) with excellent performances at room temperature. The characteristics of NDR disappeared, and transparent nonideal rectifying diodes were observed after these samples were annealed for about 30 min at 450 °C in air. Combining the studies of the x-ray photoelectron spectrum (XPS), thermogravimetric analysis (TGA), and atomic force microscopy (AFM), the role of oxygen in the NiO_x film in the determination of the characteristics of heterojunction diodes has been analyzed.

II. EXPERIMENTS

Figure 1 shows the schematic structure of the NiO_x/ITO/glass heterojunction diode. The NiO_x films of about 0.3 μm were deposited on the ITO glass by the reactive rf magnetron sputtering with different Ar/O₂ ratios in the chamber. The target was the NiO (99.99%) with a diameter of 3 in. The Ar/O₂ ratios were 100/0, 100/36, 25/100, and 0/100 for samples (a), (b), (c), and (d), respectively. The sheet resistance of the ITO glass was about 70 Ω/□. The deposition was performed at a total pressure of 20 mTorr and a rf power of 200 W. The temperature of the ITO substrates was maintained below 60 °C during sputtering. The x-ray (Cu K_α) diffraction (XRD) patterns of the NiO_x films have shown the first five peaks of the NiO lattice, which are identical to the 2θ peaks of cubic nickel oxide. The samples for TGA were obtained by scratching the films on the glass



FIG. 1. A schematic structure of the NiO_x/ITO/glass heterojunction diode. The sheet resistances of the ITO and NiO_x are 70 and (6–18) × 10⁶ Ω/□, respectively.

^{a)} Author to whom correspondence should be addressed; electronic mail: timtclu@faculty.nctu.edu.tw

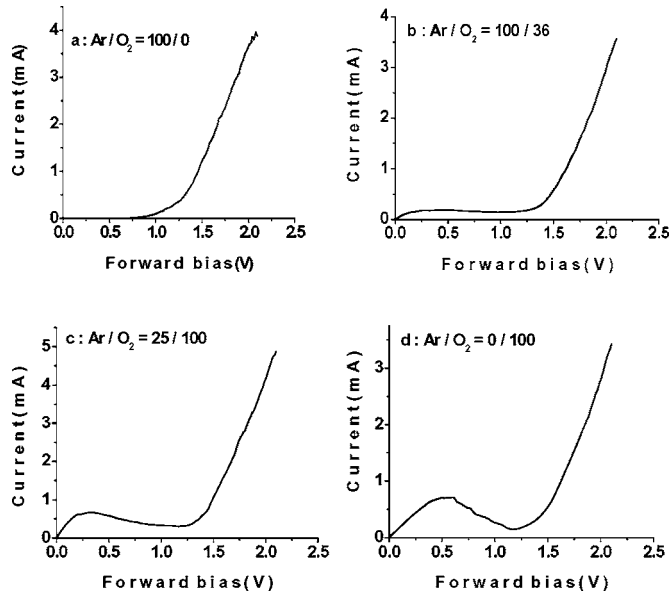


FIG. 2. Room temperature I - V curves of the $\text{NiO}_x/\text{ITO}/\text{glass}$ diodes sputtered with different gas mixing conditions before thermal annealing.

(Corning 7059). Both the films on the glass and on the ITO glass were deposited at the same conditions. Measurements of TGA were conducted under normal conditions. TGA data were also used to determine the composition of x of the NiO_x films. In addition, XPS was performed to characterize the properties of NiO_x films of the heterojunction diodes.

III. RESULTS AND DISCUSSION

Figure 2 shows the I - V curves of the as-deposited $\text{NiO}_x/\text{ITO}/\text{glass}$ heterojunctions at room temperature. The characteristics of NDR can be observed to heavily depend on the ratios of sputtering gases Ar and O_2 during the deposition of NiO_x films. From sample (a) to sample (d), the characteristics of the devices change from a rectifying diode to a diode with NDR, and both peak voltage and valley voltage increase. Apparently, the peak-to-valley current ratio (PVCR) I_p/I_v also increases from 1 to 5 when the O_2 in the gas mixture increases. In addition, the swing voltage V_s is approximately 1.05 V for every diode.

Figure 3 shows the PVCR and turn-on voltage as func-

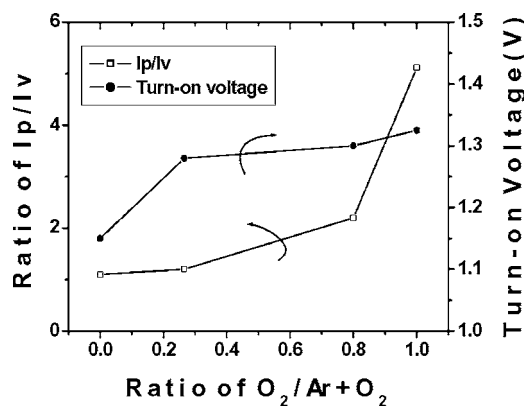


FIG. 3. Ratio of I_p/I_v and turn-on voltage of the $\text{NiO}_x/\text{ITO}/\text{glass}$ heterojunction diodes sputtered with different gas mixing ratios of $\text{O}_2/\text{Ar}+\text{O}_2$.

TABLE I. Resistivity of the NiO_x films.

Ar/ O_2 ratio	100/0	100/36	25/100	0/100
Resistivity (Ω cm)	653	303	333	170

tions of the mixture ratio of $\text{O}_2/\text{Ar}+\text{O}_2$. Both the PVCR and the turn-on voltage increase as the mixture ratio of O_2 increases. To realize the effect of O_2 in the NiO_x films, the resistivity of the NiO_x films was measured at room temperature and shown in Table I. Bransky and Tallan had reported the decrease of resistivity as the partial pressure of O_2 in the Ar- O_2 mixture increases.¹² The decreasing resistivity has been attributed to the excess O_2 in the NiO_x films causing the following reactions:



where O_O is an oxygen ion on the normal site, V_{Ni} is a nickel vacancy with two Ni^{3+} ions next to the vacancy, and V_{Ni}' and V_{Ni}'' are ionized vacancies with one and two electrons on the vacancy, respectively.^{7,12} Based on Eqs. (2) and (3), excess O_2 in the NiO_x film enhances the concentration of hole and decreases the resistivity. The increased hole concentration also increased the difference between the Fermi level of the p -type NiO_x and the fixed Fermi level of the n -type ITO.⁷ Due to the low voltage drop across the p -side NiO_x and the n -side ITO film, both built-in and turn-on voltages of the NiO_x/ITO increased as the ratio of $\text{O}_2/\text{Ar}+\text{O}_2$ increased. Since ITO is a degenerate n -type semiconductor, the depleted region is mainly on the p -side of NiO_x of the diodes.

Figure 4(a) shows the I - V curves of the $\text{NiO}_x/\text{ITO}/\text{glass}$ diodes annealed at 450°C in air for about 30 min. The characteristics of NDR disappeared and the characteristics of the rectifying diodes were observed. In the meantime, the transmittance of the rectifying diodes is over 60% and is about two times larger than the diodes with NDR at the visible region. The differential resistance also increases about ten times, from a few hundred ohms to a few thousand ohms. Sample (d) has the lowest differential resistance of about 1000–2000 Ω . As a result of high differential resistance, turn-on voltage also shifts to a higher value of 1.6–2.2 V. By investigating the I - V curves of Figs. 4(a) and 2 at a forward bias larger than the turn-on voltage, the operation current is not similar to the rapidly rising diffusion current in the conventional semiconductor p - n junctions. Instead, other factors dominate the current transport. This kind of I - V curves has been observed in the oxide-based p - n homojunctions and heterojunctions.^{13–16} In the homojunction, a linear I - V has been attributed to a change of stoichiometry in the p and n regions by increasing the voltage at high temperature.¹³ In our case, two different oxide-based materials NiO_x and ITO formed a p - n heterojunction, and a change of stoichiometry of NiO_x and ITO at room temperature could not occur. In an oxide-based p - n heterojunction, both the high series resistance and the space-charge-limited current

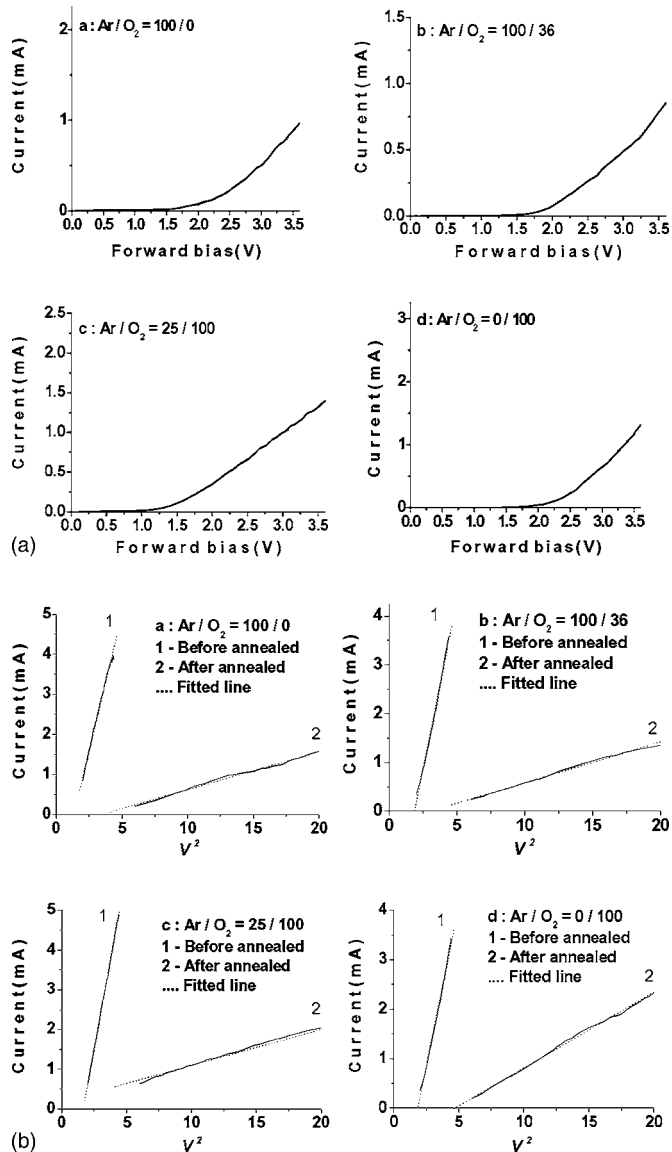


FIG. 4. (a) I - V curves of the samples (a), (b), (c), and (d) after annealing at 450 °C in air for about 30 min. Measurements were conducted at room temperature. (b) I - V^2 curves of the annealed and unannealed samples at forward bias larger than the turn-on voltage.

could be the reasons of this kind of I - V curve.^{4,14–16} The space-charge-limited current is proportional to $[(\mu V^2)/(N_t l^3)] \exp(-E_t/kT)$, where μ , V , N_t , l , and E_t are the mobility of carriers, applied voltage, density of traps, thickness of the space charge layer, and energy level of traps, respectively.^{14,17,18} Figure 4(b) shows the I - V^2 curves of samples (a)–(d) before and after annealing. Linear relations of I and V^2 were obtained for all samples at room temperature, while the forward bias voltage was larger than the turn-on voltage. The linear relation of I and V^2 indicates that the carrier transport in the NiO_x/ITO/glass heterojunction diode is dominated by the space-charge-limited current. Since ITO is a metal-like n -type semiconductor, the region of the space-charge-limited current is mainly in the p -NiO_x region. In Fig. 4(b), both space-charge-limited current and slope of I - V^2 curves decrease after annealing, where the slope is a function of N_t , l , and E_t at a fixed temperature.

To realize the changes in the characteristics of the het-

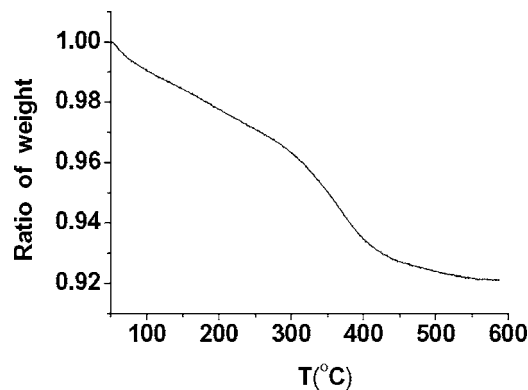


FIG. 5. Thermogravimetric analysis profile of the sample (d).

erojunction diodes before and after annealing, we inspect the characteristics of NiO_x films by XPS, TGA, and AFM. Figure 5 shows the TGA profile of sample (d) and indicates that heating NiO_x films leads to the loss of weight of NiO_x particles. As the annealing temperature was below 300 °C, the lost weight might be due to the oxygen release from the grain boundaries of nanosized NiO in the film. A clear transition appears at about 300 °C, which implies a new compound but not NiO in the NiO_x particles because the decomposed temperature of NiO is over 550 °C. While the annealing temperature is above 550 °C, the decomposition stops and the weight is retained.

Figure 6 shows XPS spectra of the NiO_x film before and after annealing. XPS spectra show two peaks at 529.5 and 532 eV. The peak of 529.5 eV represents a binding energy of O 1s peak in the NiO and the peak of 532 eV represents a binding energy of O 1s peak in the Ni₂O₃, where a nickel ion in Ni₂O₃ is Ni³⁺.^{19,20} It is known that a Ni³⁺ ion is equivalent to an acceptor and a nickel vacancy in Eqs. (2) and (3) connecting two Ni³⁺ ions via a quadruple force.⁷ On the other hand, the increasing relative content of NiO in the film indicates a chemical process connecting NiO and Ni₂O₃ while the NiO_x film is annealed. Based on the TGA results, heating causes the black NiO_x particles to decompose and change into green particles finally. Combining the results of TGA and XPS, the decomposed compound Ni₂O₃ via a reaction of $\text{Ni}_2\text{O}_3 \rightarrow 2 \text{NiO} + \frac{1}{2} \text{O}_2$ or a reaction of $\text{NiO}_x \rightarrow \text{NiO} + (x-1)/2 \text{O}_2$ in the film can produce green NiO particles and O₂. Based on Le Châtelier's principle, releasing O₂ in Eq. (1)

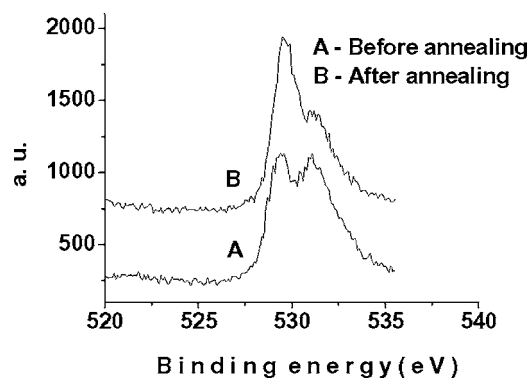


FIG. 6. X-ray photoelectron spectrum of the sample (d) before and after annealing.

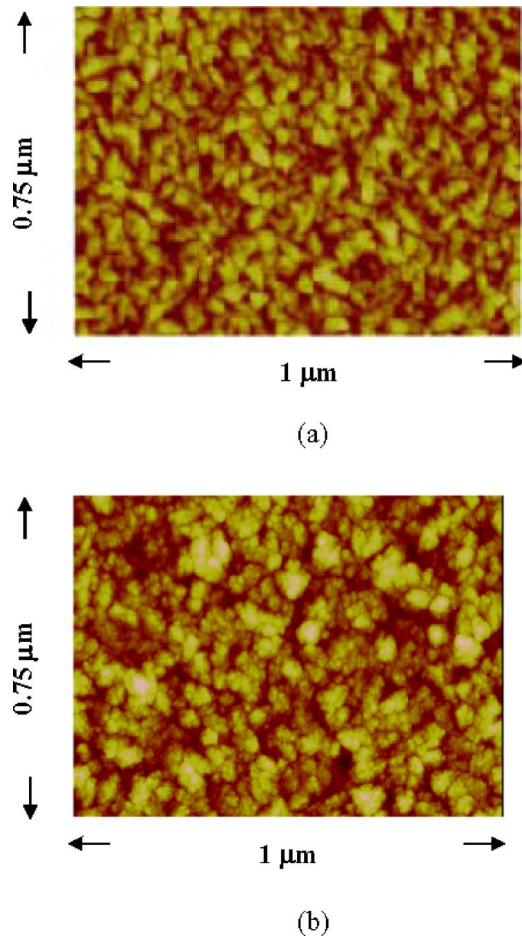


FIG. 7. (Color online) (a) AFM images of the sample (d) before annealing and (b) after annealing.

causes the concentration of holes or Ni^{3+} ions to decrease, which is responsible for the increase of the resistance and turn-on voltage of the heterojunction diodes. Besides, the Ni^{3+} ion is also a color center in the film,²¹ where the lower concentration of Ni^{3+} ions increases the transmittance of rectifying diodes.

Figures 7(a) and 7(b) show the AFM images of the NiO_x film on the ITO glass before and after annealing, respectively. In Fig. 7(a), the film composed of grains with size of about 30 nm shows clear boundaries. The XRD analysis indicated that crystallite NiO was embedded in the grains and TGA showed the excess oxygen in the film. On the other hand, XPS showed two states of oxygen in the film, i.e., NiO and Ni_2O_3 . The results of XRD and XPS indicated that the excess oxygen had to be located between grain boundaries of NiO forming V_{Ni}' and V_{Ni}'' vacancies, as shown in Eqs. (2) and (3). As is well known, semiconductor grain boundaries formed a double Schottky barrier with a space-charge region along the boundaries.²² In Fig. 4(b), the space-charge-limited current is the evidence that holes transport across the boundary region. In Fig. 7(b), the grain structure of NiO_x is similar to Fig. 7(a), but the shape of the grains is different and the size of the grains increases. The space between grain boundaries was also enlarged when the sample was annealed. The increased size of the crystallite NiO was consistent with the XRD analysis that the full width at half maximum (FWHM)

of NiO 2θ peaks was narrowed. The increased grain size could be the result of grains merging together due to the excess oxygen released between grain boundaries. After oxygen was released, the decreased hole concentration caused the space-charge-limited current and slopes shown in Fig. 4(b) to decrease since the space-charge-limited current is proportional to free carriers.¹⁷

Since the energy states of V_{Ni}' in the NiO_x were higher than the Fermi level,⁷ the property of the NiO_x was analogous to a p^+ -type (degenerate) semiconductor. Therefore, the p^+-n^+ heterojunction structure of $\text{NiO}_x/\text{ITO}/\text{glass}$ could be the cause NDR at small forward bias since the electrons at the ITO side could tunnel to the finite energy states of V_{Ni}' . After oxygen was released from the NiO_x film, the decreased concentration of V_{Ni}' , as shown in Eq. (2), caused the disappearance of the NDR.

Results of TGA, XPS, AFM, and XRD indicated that oxygen in the NiO_x film was responsible for the characteristic changes. Furthermore, the depleted region of the diode was mainly on the NiO_x layer. Therefore, decreasing oxygen content in the NiO_x layer leads both to the disappearance of NDR characteristics and to the decrease in the space-charge-limited current as well as the slope of the $I-V^2$. In the meantime, the diodes with higher transmittance and higher differential resistance are also due to the released oxygen content.

IV. CONCLUSIONS

$p\text{-NiO}_x/n\text{-ITO}/\text{glass}$ heterojunction diodes were demonstrated. The ratios of sputtering gaseous Ar and O_2 during the NiO_x film were formed and heavily changed the characteristics of the heterojunction diodes from rectifying diodes to diodes with NDR. After annealing at 450 °C in air for about 30 min, all diodes showed properties with higher transmittance and differential resistance in comparison with the diodes before annealing. Linear $I-V^2$ curves indicated that the space-charge-limited current dominates the current transport in the NiO_x layer. By analyzing the properties of NiO_x films with XPS spectra, TGA data, and AFM image, the released oxygen in the NiO_x films was found to be responsible for the disappearance of NDR characteristics and the for the change of the nonideal rectifying diode characteristics. The results should be useful and helpful in optimizing the process of the transparent oxide-based heterojunction diodes.

ACKNOWLEDGMENTS

This work was supported in part by the National Science Council of the Republic of China (ROC) in Taiwan under Contract No. NSC93-2120-M-009-006 and by the Academic Excellence Program of the ROC Ministry of Education under Contract No. NSC93-2752-E-009-008-PAE.

¹N. Miura, J. Wang, M. Nakatou, P. Elumalai, and M. Hasei, *Electrochem. Solid-State Lett.* **8**, H9 (2005).

²H. Ohta, K. Kawamura, M. Orita, M. Hirano, N. Sarukura, and H. Hosono, *Appl. Phys. Lett.* **77**, 475 (2000).

³R. L. Hoffman, B. J. Norris, and J. F. Wager, *Appl. Phys. Lett.* **82**, 733 (2003).

⁴X. L. Guo, J. H. Choi, H. Tabata, and T. Kawai, *Jpn. J. Appl. Phys., Part 2* **40**, L177 (2001).

⁵H. Ohta, M. Hirano, K. Nakahara, H. Maruta, T. Tanabe, M. Kamiya, T.

- Kamiya, and H. Hosono, *Appl. Phys. Lett.* **83**, 1029 (2003).
- ⁶W. Y. Lee, D. Mauri, and C. H. Wang, *Appl. Phys. Lett.* **72**, 1584 (1998).
- ⁷D. Adler and J. Feinleib, *Phys. Rev. B* **2**, 3112 (1970).
- ⁸A. Kudo, H. Yanagi, K. Ueda, H. Hosono, and H. Kawazoe, *Appl. Phys. Lett.* **75**, 2851 (1999).
- ⁹H. Kawazoe, M. Yasukawa, H. Hyodo, M. Kurita, H. Yanagi, and H. Hosono, *Nature (London)* **389**, 939 (1997).
- ¹⁰A. Kudo, H. Yanagi, H. Hosono, and H. Kawazoe, *Appl. Phys. Lett.* **73**, 220 (1998).
- ¹¹H. Sato, T. Minami, S. Takata, and T. Yamada, *Thin Solid Films* **236**, 27 (1993).
- ¹²I. Bransky and N. M. Tallan, *J. Chem. Phys.* **49**, 1243 (1968).
- ¹³I. Riess, *Phys. Rev. B* **35**, 5740 (1987).
- ¹⁴M. Sugiura, K. Uragou, M. Tachiki, and T. Kobayashi, *J. Appl. Phys.* **90**, 187 (2001).
- ¹⁵T. Nakasaka, K. Urago, M. Sugiura, and T. Kobayashi, *Jpn. J. Appl. Phys., Part 2* **40**, L518 (2001).
- ¹⁶G. Z. Yang, H. B. Lu, F. Chen, T. Zhao, and Z. H. Chen, *J. Cryst. Growth* **227–228**, 929 (2001).
- ¹⁷A. Rose, *Phys. Rev.* **97**, 1538 (1955).
- ¹⁸R. H. Jarman, *J. Appl. Phys.* **60**, 1210 (1986).
- ¹⁹A. Agrawal, H. R. Habbi, R. K. Agrawal, T. P. Cronin, D. M. Roberts, S. Caron-Popowich, and C. M. Lampert, *Thin Solid Films* **221**, 239 (1992).
- ²⁰K. S. Kim and N. Winograd, *Surf. Sci.* **43**, 625 (1974).
- ²¹M. Kitao, K. Izawa, K. Urabe, T. Komatsu, S. Kuwano, and S. Yamada, *Jpn. J. Appl. Phys., Part 1* **33**, 6656 (1994).
- ²²C. R. M. Grovenor, *J. Phys. C* **18**, 4079 (1985).